







The Impact of Shear Reinforcement Amount and Arrangement on the Shear Capacity of Shallow RC Beams: An Experimental Study

Ahmed A. Soliman^{1, 2*} , Dina M. Mansour¹ , Ayman H. Khalil² , Ahmed Ebid¹ 

¹ Structural Engineering & Construction Management Department, Faculty of Engineering & Technology, Future University in Egypt, Egypt.

² Structural Engineering Department, Faculty of Engineering, Ain Shams University, Egypt.

Received 07 August 2023; Revised 11 November 2023; Accepted 19 November 2023; Published 01 December 2023

Abstract

This study investigates the impact of shear reinforcement amount and arrangement on the shear capacity of shallow/wide RC beams. Seven specimens of shallow/wide beams with different ultimate shear reinforcement stress ($\mu.F_{ys}$), longitudinal spacing to depth ratio (S/d), and transversal spacing to depth ratio (S'/d) were tested under a monotonic three-point bending test. All the specimens were designed to fail at shearing. The results showed that the shear reinforcement was fully functioning until it yielded; also, the amount of shear reinforcement had the major impact on the shear capacity; in addition, the transverse spacing had more influence on the shear capacity than the longitudinal spacing. The measured shear capacities were compared to six design codes, in which the results ranged from 95% to 110%, with the Japanese code (JSCE) being the closest to the experimental results. Two AI-based predicting equations, "Genetic Programming" (GP) and "Evolutionary Polynomial Regression" (EPR), were also compared to the experimental, with accuracies of 78% and 86% of the measured capacities, respectively. Initial stiffness, final stiffness, dissipated energy, and ductility were all discussed for the seven specimens, with ultimate shear reinforcement stress being the most impactful on the total shear capacity of the wide beams.

Keywords: Wide Beams; Shallow Beams; Stirrups Spacing; Shear Capacity; Genetic Programming; Evolutionary Polynomial Regression.

1. Introduction

Wide-shallow beams have been widely used in architectural applications due to their aesthetic appeal and structural efficiency. However, the shear behavior of wide-shallow beams is a complex issue that has been the subject of much research. The shear capacity of these beams has been affected by several factors, including the longitudinal spacing between stirrups, the spacing between the stirrup legs, and the shear reinforcement ratio. The contribution of shear reinforcement and the presence of stirrups in wide beams were ignored by early code provisions, even though research on the shear behavior of wide beams began several decades ago. Wide beams were defined by several researchers as beams with widths that are twice their depths [1, 2]. The gaps in the research on wide beams have been gradually filled over time as more and more parameters and variables have been discussed. Most of the studies mentioned were experimental and were backed up by finite element analysis.

Soliman et al. [3] had investigated the shear capacity of seven wide-shallow beam specimens, considering the aspect ratio, concrete compressive strength, and ratio of compression rebar. The ultimate shear strength of the specimens decreased when the aspect ratio increased from 1.66 to 5. The shear capacity of the beams increased when the compressive strength increased, but the increase in compression rebar had a small impact on the shear capacity of the

* Corresponding author: ahmed.soliman@fue.edu.eg

 <http://dx.doi.org/10.28991/CEJ-2023-09-12-013>



© 2023 by the authors. Licensee C.E.J, Tehran, Iran. This article is an open access article distributed under the terms and conditions of the Creative Commons Attribution (CC-BY) license (<http://creativecommons.org/licenses/by/4.0/>).

beams. Concrete compressive strength was always the first parameter considered for wide beams, as investigated by Serna et al. [4]. Wang et al. [5] had used engineered composite concrete as an outside external strengthening layer, which enhanced the shear capacity of the wide beams and their crack pattern. The depth of wide beams was investigated by Morsy et al. [6], who advised an optimum depth of 250 mm for stirrup usage. Taha & Abbas [7] had considered the spacing between stirrups as a percentage of the depth of the wide beams.

De Sousa et al. had investigated the shear strength of wide concrete members without stirrups, their failure mechanisms, and their transition of failure mechanisms from shear to punching. It was stated that the width-to-depth ratio (b/d) of the concrete members did not affect the crack pattern as much as the member slenderness and reinforcement ratio [8–10]. Also, increasing the reinforcement in the wide members changed the failure mechanism in these members compared to failures due to the yielding of the reinforcement (longitudinal and transverse), causing it to be a brittle failure. Moreover, a correction factor was introduced to account for the presence of the shear reinforcement in the wide members under concentrated loads, which enhanced the precision of the expression in the ACI 318-19.

Several steel configurations other than conventional stirrups were investigated. Moubarak et al. [11] introduced internal and external fasteners as a shear-resisting system for wide beams, which significantly increased the shear capacity of the beams. Elansary et al. [12] had used a spiral reinforcement system embedded in the wide beams, which increased the ductility of the beams. Moahammed et al. [13] used steel plates with holes in them as a replacement for the stirrups, which had a very small impact on the total shear capacity of the wide beams.

The width of the supports was investigated by Khalil et al. [14], who found that as the supports got narrower, the less shear capacity and flexure they endured. An experimental program was conducted by Mahmoud et al. [15], who found that as the eccentricity increased, the shear capacity of the wide beams decreased.

The use of FRP was always a point of research. Ebid & Deifalla [16] had collected massive data on concrete beams, both conventional and wide, all reinforced with FRP bars. An equation for shear was developed that showed better results than the equations already present in some codes. Shear behavior of one-way slabs reinforced by FRP was investigated by Abdul-Salam et al. [17] and Al-Harmany et al. [18], who both confirmed the increase in the shear capacity of the specimens, but their failures were brittle. El-Sayed et al. [19] tested reinforced concrete wide beams with external CFRP plates, which increased the shear capacity of the beams. However, all the specimens had a debonding failure. Conforti et al. [20] used polypropylene fiber reinforcement in their experimental investigation of the wide, shallow beams. The ductility of the specimens increased as the volume fraction was considered optimal.

The usage of recycled concrete aggregates has been used in concrete members for the last several years, and its effect on the shear strength of the concrete beams has been investigated by several research teams lately. Odero et al. [21] tested sixteen concrete beams using RCA and concluded that at 10 mm aggregates, the shear capacity of the specimens was at its highest by 21.5%. Sagheer et al. [22] had tested fifteen concrete beams with 50 % RCA for some and 100 % RCA for the others. The specimens with 100 had a 26% increase in their shear capacity compared to the 50 % RCA. Engineered cementitious composites were used to enhance the shear strength of concrete beams without using stirrups by Cheng et al. [23]. The shear capacity and toughness were both improved for the concrete beams. Yu et al. [24] had used ANN and RF machine learning models on 264 RCA beams (collected test results), and it was stated that these models had better predictive outputs for RCA beams than other existing models.

One-way shear-reinforced concrete slabs were heavily investigated by Lantsoght et al. [25, 26]. The shear capacity of one-way slabs, one-way slabs under concentrated loads, one-way slabs without shear reinforcement, and one-way slabs under different combinations of loads were all carefully considered for these studies. The behavior of the one-way slabs was in accordance with what was recorded through several studies of the reinforced concrete shallow-wide beams. Alluqmani [27] compared the experimental results of wide beams with web reinforcement to the guidelines of the Saudi Code and Euro Code 2. The Saudi Code was found to be safer than the Euro Code.

The recent advancements in artificial intelligence and machine learning have led to new research opportunities in the field of concrete elements. Several recent studies have used machine learning to predict the shear capacity and mode of failure of reinforced concrete beams [28–31]. The results of these studies suggest that machine learning is a promising approach for predicting the behavior of concrete elements [32].

Soliman et al. [33] identified several gaps in the previous studies and investigations regarding the shear capacity of the wide, shallow reinforced concrete beams. Most previous studies had, of course, focused on the stirrup configurations at the shallow-wide beams, as the code provisions and expressions were completely negligible for the matter as mentioned before. But the contribution of the shear reinforcement to the total shear capacity of the wide beams was not investigated considering the transverse spacing of the stirrup's branches to the depth ratio (S'/d) and the ultimate shear reinforcement stress ($\mu.F_{ys}$), which leaves a lot of room for research.

2. Objectives

The main objective of this research is to experimentally investigate the impact of longitudinal spacing of stirrups to depth ratio (S/d), transverse spacing of stirrup's branches to depth ratio (S'/d), and the ultimate shear reinforcement stress ($\mu.F_{ys}$) on the structural behavior of shallow/wide RC beams in terms of failure mode, first crack, shear capacity, beam stiffness, and ductility, and finally, assessing the shear design provisions in six different design codes. The methodology used is illustrated in Figure 1.

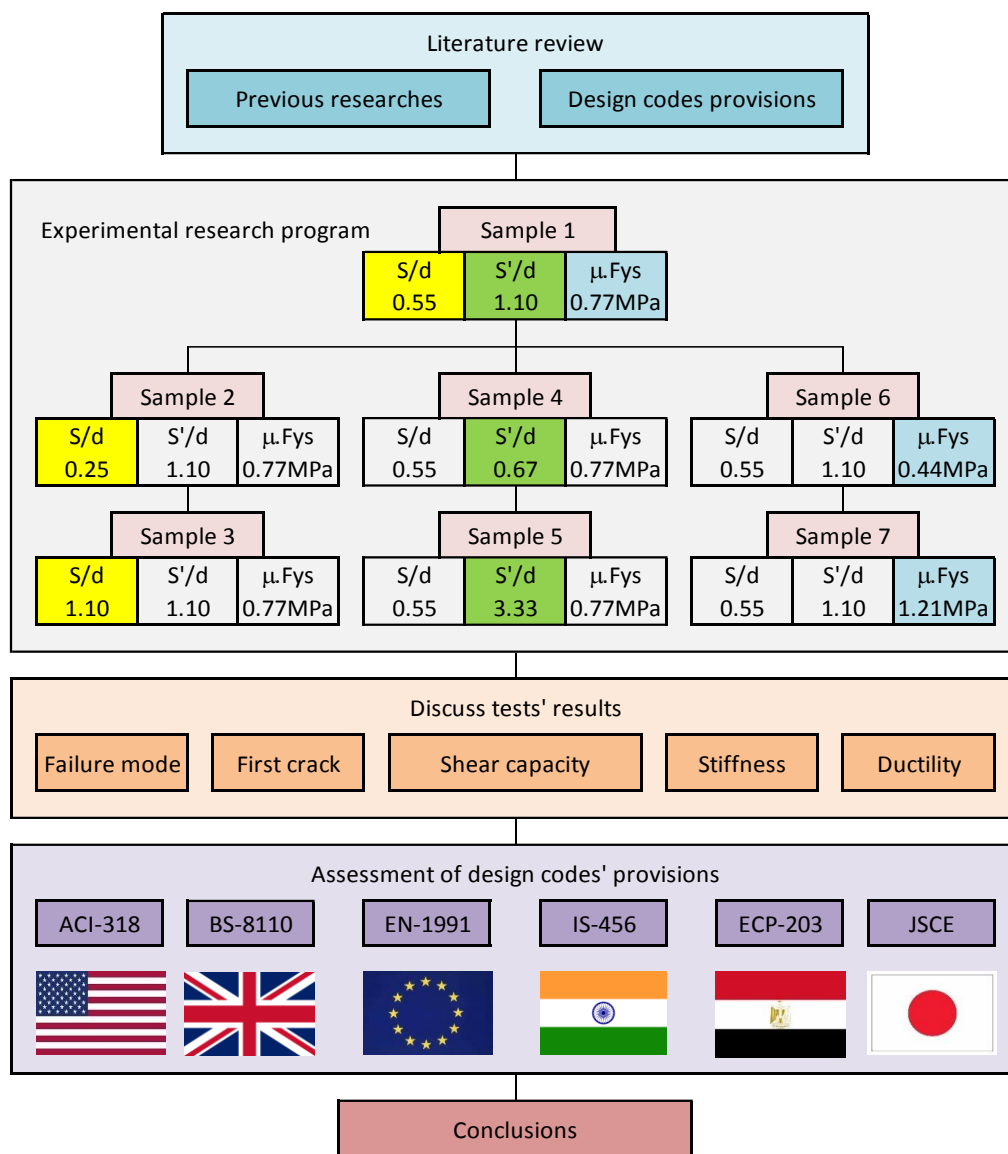


Figure 1. The research methodology

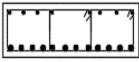
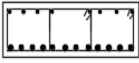


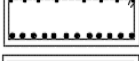
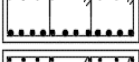
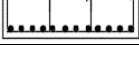
3. Experimental Program and Methodology

3.1. Samples Configurations

The experimental research program consisted of seven RC beams with the same dimensions (1200 x 600 x 200 mm), same material ($F_c=31$ MPa), the same lower reinforcement ($A_s = 12T18$, $F_y = 416$ MPa) and the same upper reinforcement ($A_s'=8T10$, $F_y=416$ MPa). All the beams were tested up to failure in a three-point bending test with a span of (1050 mm) which is equivalent to (shear span/depth) ratio of ($525/180=2.9$). The impact of each studied parameter was investigated using three wide beam specimens as follows:

The effect of longitudinal spacing of stirrups to depth ratio (S/d) was studied using specimens B1, B2, and B3. Each specimen had ($S'/d=1.10$), ($\mu.F_{ys}= 0.77$ MPa) but ($S/d= 0.55, 0.25$, and 1.10) respectively. The influence of the transverse spacing of stirrup's branches to the depth ratio (S'/d) was explored with specimens B1, B4, and B5, where all of them had ($S/d=0.55$), ($\mu.F_{ys}= 0.77$ MPa) but ($S'/d= 1.10, 0.67$, and 3.33) respectively. Finally, the impact of ultimate shear reinforcement stress ($\mu.F_{ys}$) was investigated by beams B1, B6, and B7, where all of them had ($S/d=0.55$), ($S'/d=1.10$) but ($\mu.F_{ys}= 0.77, 0.44$ and 1.21 MPa) respectively. Table 1 summarizes the configurations of all tested samples.

Table 1. The configurations of all tested samples

Beam ID	Cross section	Stirrups details	(S) mm	(S') mm	(μ)%	(F_{ys}) MPa	(S/d) - (S'/d)-	($\mu.F_{ys}$) MPa
B1		4R8-100	100	200	0.33	233	0.55 1.10	0.77
B2		4R6-45	45	200	0.33	233	0.28 1.10	0.77
B3		2x4R8-200 (Double stirrup)	200	200	0.33	233	1.10 1.10	0.77
B4		2R8+4R6-100	100	120	0.33	233	0.55 0.67	0.77
B5		2x4R8-100 (Double stirrup)	100	600	0.33	233	0.55 3.33	0.77
B6		4R6-100	100	200	0.19	233	0.55 1.10	0.44
B7		4T10-100	100	200	0.52	233	0.55 1.10	1.21

3.2. Test Setup and Instrumentation

All seven wide beam specimens were tested to failure using a monotonic load through a three-point bending test. The testing took place within a concrete laboratory at El Shorouk Academy in El Shorouk City, Egypt. Within the laboratory, a testing setup was established, featuring a 1000 KN hydraulic jack as depicted in Figure 2-b. During the testing process, the specimens were positioned within the testing frame. Two cylindrical steel bars were used as supports. One of these bars was fixed to a base plate to replicate a hinged support, while the other steel bar remained unfixed, serving as a roller support. The midpoints of the specimens were aligned beneath the hydraulic jack. To transfer the load from the jack to the beam, a distributing steel beam was deployed, transforming the point load from the jack into a distributed load on the beam. The configuration of the test setup is visually represented in Figure 2-a.

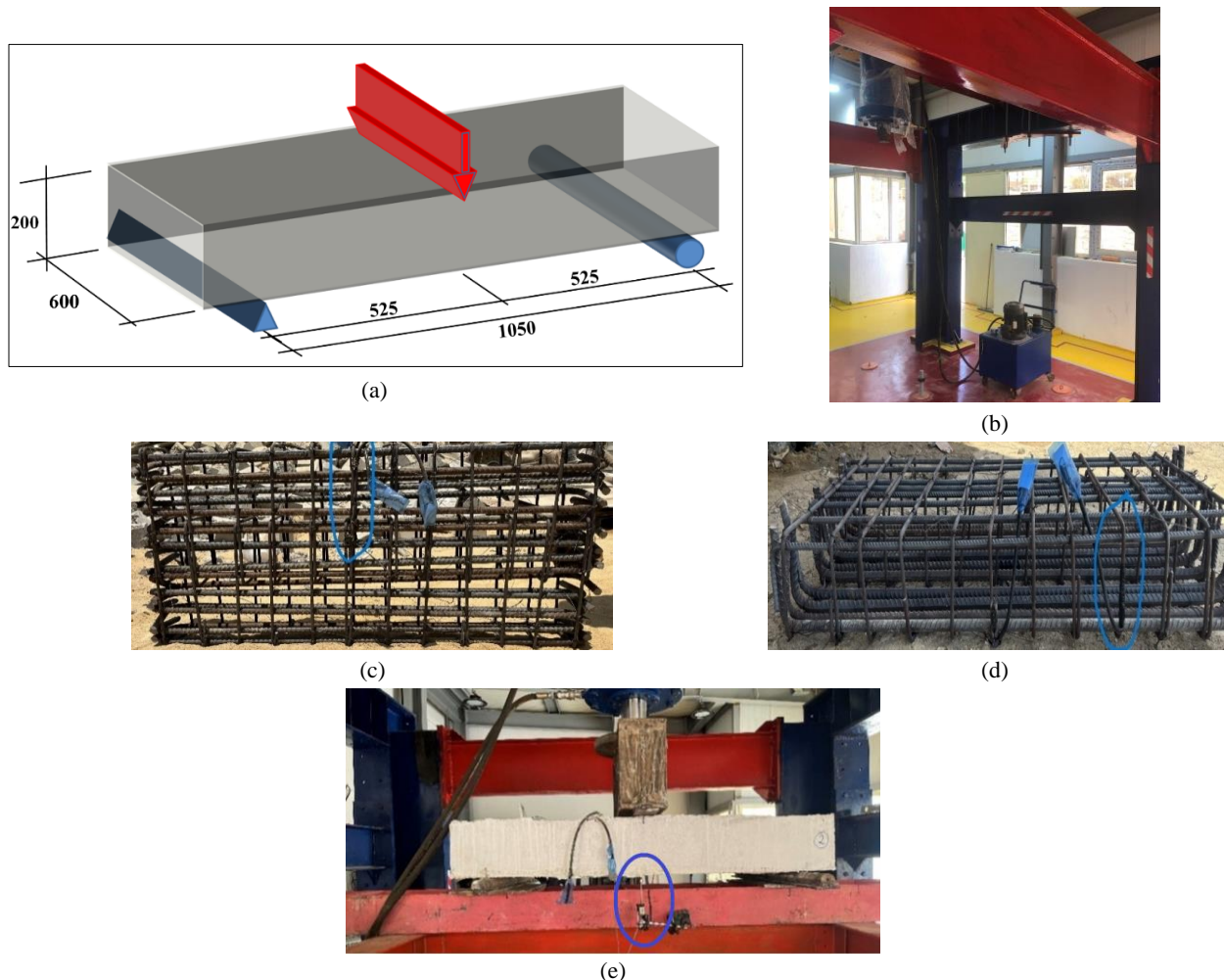


Figure 2. Samples instrumentation and test configurations, a) test setup, b) testing frame, c) longitudinal rebars strain gauge, d) stirrups strain gauge, e) LVTDs locations

Each tested beam was equipped with two strain gauges. One strain gauge was positioned at the midpoint of the central longitudinal tension rebar, while the other was located on the outer branch of the stirrup, approximately 100 mm from the support. The purpose of the first strain gauge was to identify the flexural failure mode, whereas the second strain gauge was used to identify the failure mode. Additionally, the mid-span deflection of the specimens was measured using two LVTDs (Linear Variable Differential Transformers), placed beneath the beam on its front and back sides. Finally, the load applied during the testing of the specimens was measured using a load cell attached to the hydraulic jack. Throughout the entire testing process, all measurements were automatically recorded by a data acquisition system. Figures 2-c, 2-d, and 2-e provide a visual representation of the locations of the strain gauges and LVTDs.

4. Test Results

The data acquisition system had automatically logged the applied load, mid-span deflection, and strain measurements in both ties and tension rebars for all the tested specimens of the wide-shallow beams. Additionally, visual observation and documentation of crack patterns, their locations, orientations, and propagation were conducted on the samples. The wide-shallow beams were subjected to strain-controlled loading at a rate of 1.0 mm/min. The initial flexural crack on the lower surface of each specimen was identified, and the corresponding load and deflection values were recorded. Subsequently, the applied load was progressively increased until the point of failure. Figure 3 illustrates the load-deflection curves that were recorded up to the failure loads (maximum loads). Furthermore, Table 2 provides a summary of the recorded values, encompassing the load and deflection measurements at the first crack stage and the ultimate stage, along with the ultimate strains present in both ties and tension rebars. The final column in the table showcases photographs depicting the observed crack patterns.

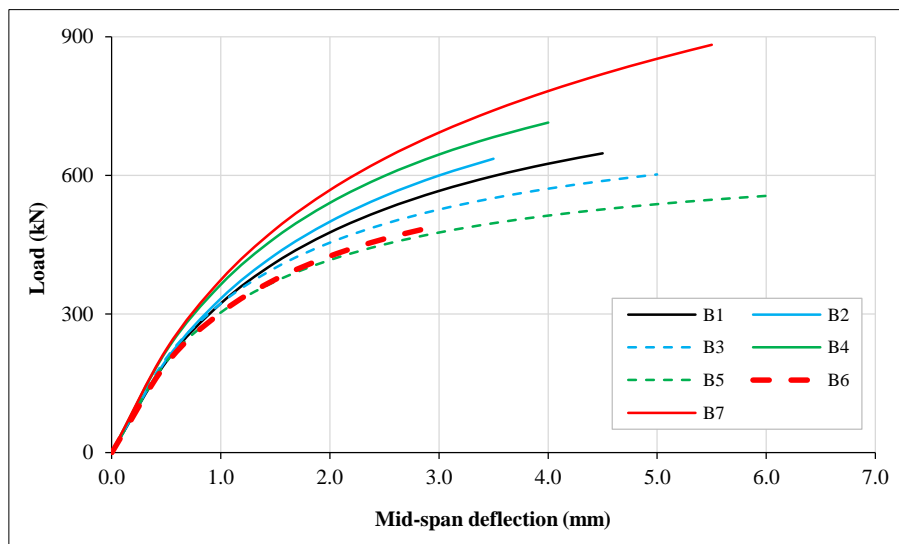


Figure 3. Load - Deflection curve of the tested wide beams specimens

Table 2. Experimental program results including cracking and ultimate loads, cracking and ultimate deflections, and strain measured in ties and rebars

Beam ID	Crack pattern	Pcr (KN)	Pu (KN)	Δ_{cr} (mm)	Δ_u (mm)	$\epsilon_{u, sh}$ ($\mu\epsilon$)	ϵ_u ($\mu\epsilon$)
B1		88	660	0.22	4.50	1930	1650
B2		90	640	0.21	3.50	1750	1820
B3		83	600	0.23	5.00	2251	1568
B4		88	690	0.20	4.00	2948	1800
B5		88	550	0.24	6.00	2795	1835
B6		80	490	0.25	3.00	1650	1252
B7		100	880	0.23	5.50	2050	1600

5. Discussion

5.1. Mode of Failure

All the tested beams exhibited similar behavior throughout the testing process. Initially, vertical flexural cracks initiated on the lower surface of the beams at their mid-span. The quantity and width of these cracks increased progressively as the load was applied. At a certain point, diagonal cracks emerged, connecting the load with the applied point and the supporting points. These diagonal cracks were extended in length and width until the eventual failure of the beams; the details can be found in Table 2. The failure modes that were observed in all cases were characterized by gradual and ductile behavior, lacking sudden changes, as visually depicted in Table 2.

Visual observations strongly suggested that the failure mechanism for all beams was primarily due to shear stress. Analyzing the maximum strain values listed in Table 2 revealed that the strain in the tension rebars had remained below their yield strain ($\epsilon_y = F_y/E_s = 416/200\,000 = 2080 \mu\text{-strain}$). This observation indicated that the specimens did not experience failure due to bending. Conversely, the strain values in the ties surpassed the yield strain ($\epsilon_{ys} = F_{ys}/E_s = 233/200\,000 = 1165 \mu\text{-strain}$), implying that the failure of all specimens had occurred due to shear stress.

Comparing the results of specimens B1, B2, and B3, it was indicated that crack density increases with increasing (S/d), although they all almost had the same failure load.

5.2. First Crack Width

The initial crack loads for the tested wide-shallow beam specimens were recorded in Table 2. These loads were primarily influenced by the specimen's cross-sectional dimensions, the tensile strength of the concrete, and, to a minor extent, the reinforcement ratio. Consequently, it's logical that all tested beams exhibited nearly identical first crack loads. The theoretical first crack load is about 92 kN (considering $F_t = 0.6 \sqrt{F_c'}$), which almost equals the measured values except for three samples: B3 (Pcr = 83 kN & S/d = 1.10), B6 (Pcr = 80 kN & $\mu = 0.19\%$), and B7 (Pcr = 100 kN & $\mu.F_{ys} = 1.21 \text{ MPa}$). These results indicated that increasing the (S/d) from 0.55 to 1.10 decreases the first crack load by 10%, decreasing the shear reinforcement ratio (μ) to the minimum allowed value decreases the first crack load by 13%, and finally, increasing the ultimate shear reinforcement stress to almost five times the minimum value increases the first crack load by 8%. Figure 4 presents the relationship between the theoretical and experimental first crack loads.

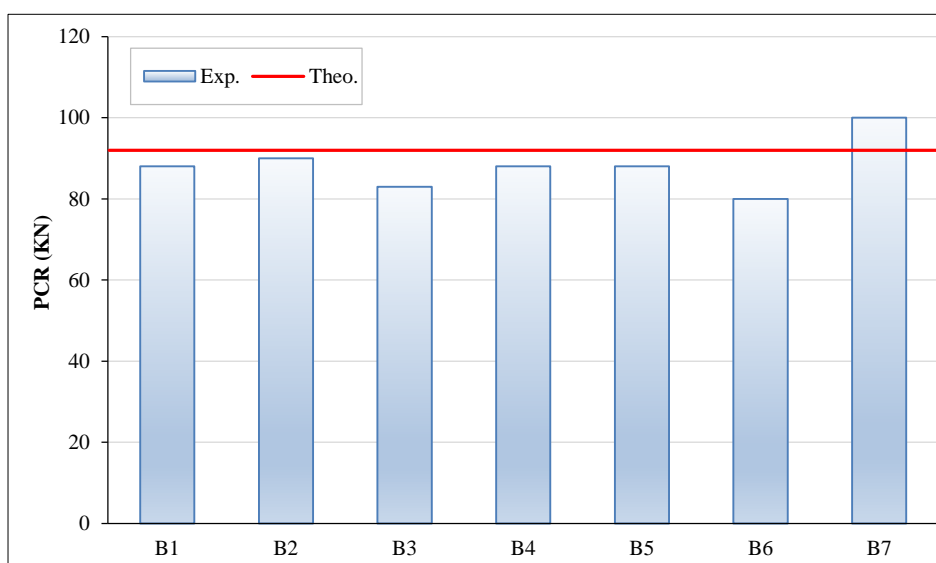


Figure 4. Experimental and theoretical first crack load values of tested beams, (kN)

5.3. Shear Capacity

Figure 5-a illustrates the relationship between the total shear strength (v_u) and (S/d). It was clear that using longitudinal spacing between the stirrups (S) larger than (0.5d) had reduced the shear strength. On the other hand, the unexpected reduction in shear strength at S/d = 0.28 may be because of some internal voids or honeycombs due to the very narrow spacing between stirrups (only 45 mm). Similarly, Figure 5-b shows the relation between (S'/d) and (v_u), which also indicated that using transverse spacing between the stirrup's branches with a value greater than (0.5d) had reduced the shear strength of the specimens. Besides that, two more points could be noted. The first is that both fitting equations showed the same theoretical (v_u) value at zero spacing (3.33 MPa). The second note is that the slope of the fitting line of (S) is twice that of (S'), which means that the reduction effect of the longitudinal spacing is twice the effect of the transverse spacing.

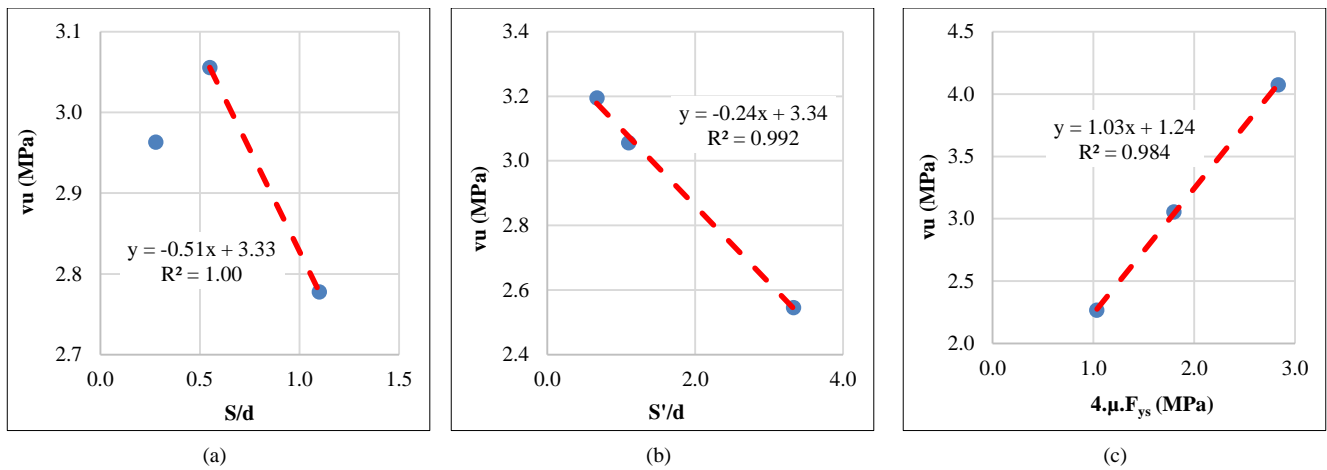


Figure 5. Total shear strength (vu) Vs a) (S/d), b) (S'/d), and c) Shear reinforcement strength

The total shear capacities (Vu) of the tested beams are equal to half the ultimate load values (Pu) mentioned in Table 4, and the ultimate total shear strength (vu) is the ultimate capacity divided by the cross-section area (vu = Vu/b.d). This shear strength is the sum of the concrete contribution (vc), longitudinal rebar contribution (vp), and shear reinforcement contribution (vs) as follows:

$$vu = vc + vp + vs \tag{1}$$

Since all the tested beams have the same dimensions, concrete strength, and longitudinal rebars, they all have the same concrete contribution and longitudinal rebar contribution (vc+vp), and only the shear reinforcement contribution (vs) is responsible for the difference in total shear strengths. Plotting the total shear strength (vu) of beams B1, B6, and B7 against their theoretical ultimate shear reinforcement strength (4 stirrups × Ash.fys) as shown in Figure 5-c showed that (vc+vp) equals 1.24 MPa for all the samples, which matches the results of the first part of this research [3]. The difference between (vu) and (1.24 MPa) is (vs).

5.4. Comparison with Codes of Practice and Previous Studies

Both total shear strength and shear strength contributed by the shear reinforcement (vu & vs) of the tested beams were calculated using the formulas from six of the most used codes of practice, besides, two (AI) predictive models obtained from previous studies as shown in Table 3. Both experimental and calculated values of (vu & vs) for all tested beams are evaluated and summarized in Table 4 and graphically presented in Figures 6 to 8.

Table 3. Shear strength formulas for different design codes and (AI) prediction models

Code	Ult. Shear strength of concrete $vc = Vc/(b.d)$	Ult. Shear strength of Stirrups $vs = Vs/(b.d) = \mu.F_{ys}$
ACI 318 [34]	$0.16 (F_c')^{0.5} + 17 \rho$	$F_{ys} \cdot A_{sh} / (S.b)$
BS 8110 [35]	$0.79(100 \rho)^{0.33}(400/d)^{0.25} (F_{cu}/25)^{0.33}$	$0.95 F_{ys} \cdot A_{sh} / (S.b) \cdot [1 - (d'/d)]$
EN-1991[36]	$0.18 [(1+(200/d))^{0.5} (100 \rho F_c')^{0.33}$	$0.9 F_{ys} \cdot A_{sh} / (S.b)$
IS 456 [37]	1.5 vc (From table)	$F_{ys} \cdot A_{sh} / (S.b)$
ECP-203[38]	$0.16 (F_{cu})^{0.5}$	$F_{ys} \cdot A_{sh} / (S.b)$
JSCE [39]	$0.2(1000/d)^{0.25}(1000 \rho)^{0.33} (F_c')^{0.33}$	$0.9 F_{ys} \cdot A_{sh} / (S.b)$
Ref.	Formula	
GP [40]	$Vu = \frac{1.25 \text{Ln} (1.3 + 0.7\mu_{sh} \cdot f_{ys} + 0.2 \cdot \rho)}{\text{Ln} (45(a/d)(E_c/E_s))} \cdot b \cdot d \cdot \sqrt{f_c'}$	
EPR [41]	$Vu = \frac{d(64 \rho - 24d + 6.8) - a(234b \cdot \rho + 1) - 0.11}{b \cdot d} + \frac{154a - 1080d + 66.5}{d \cdot f_c'} + \frac{a}{1.75d^2} + \frac{d(694 d + 370 b - 1317 \rho) - 11}{a} - \frac{b}{2.75\rho} - \frac{f_c'^2}{580} + 128 b^2 - 78.5 d^2 + 31.9 a + 19\rho (360 b + 150 d + f_c' - 950 \rho) - 22.5$	

Table 4. Experimental and calculated concrete, reinforcement & total ultimate shear strength

Code	Beam	B1	B2	B3	B4	B5	B6	B7
Exp.	vc	1.24	1.24	1.24	1.24	1.24	1.24	1.24
	vs	1.82	1.72	1.54	1.95	1.31	1.03	2.83
	vu	3.06	2.96	2.78	3.19	2.55	2.27	4.07
ACI 318	vc	1.37	1.37	1.37	1.37	1.37	1.37	1.37
	vs	1.80	1.80	1.80	1.80	1.80	1.04	2.84
	vu	3.17	3.17	3.17	3.17	3.17	2.41	4.21
BS 8110	vc	1.58	1.58	1.58	1.58	1.58	1.58	1.58
	vs	1.52	1.52	1.52	1.52	1.52	0.87	2.39
	vu	3.10	3.10	3.10	3.10	3.10	2.45	3.97
EN-1991	vc	1.16	1.16	1.16	1.16	1.16	1.16	1.16
	vs	1.62	1.62	1.62	1.62	1.62	0.93	2.55
	vu	2.78	2.78	2.78	2.78	2.78	2.09	3.71
IS-456	vc	1.43	1.43	1.43	1.43	1.43	1.43	1.43
	vs	1.80	1.80	1.80	1.80	1.80	1.04	2.84
	vu	3.23	3.23	3.23	3.23	3.23	2.47	4.27
ECP-203	vc	1.00	1.00	1.00	1.00	1.00	1.00	1.00
	vs	1.80	1.80	1.80	1.80	1.80	1.04	2.84
	vu	2.80	2.80	2.80	2.80	2.80	2.04	3.84
JSCE	vc	1.41	1.41	1.41	1.41	1.41	1.41	1.41
	vs	1.62	1.62	1.62	1.62	1.62	0.93	2.55
	vu	3.03	3.03	3.03	3.03	3.03	2.34	3.96
GP	vu	2.30	2.30	2.30	2.30	2.30	1.73	2.91
EPR	vu	2.50	2.50	2.50	2.50	2.50	2.50	2.50

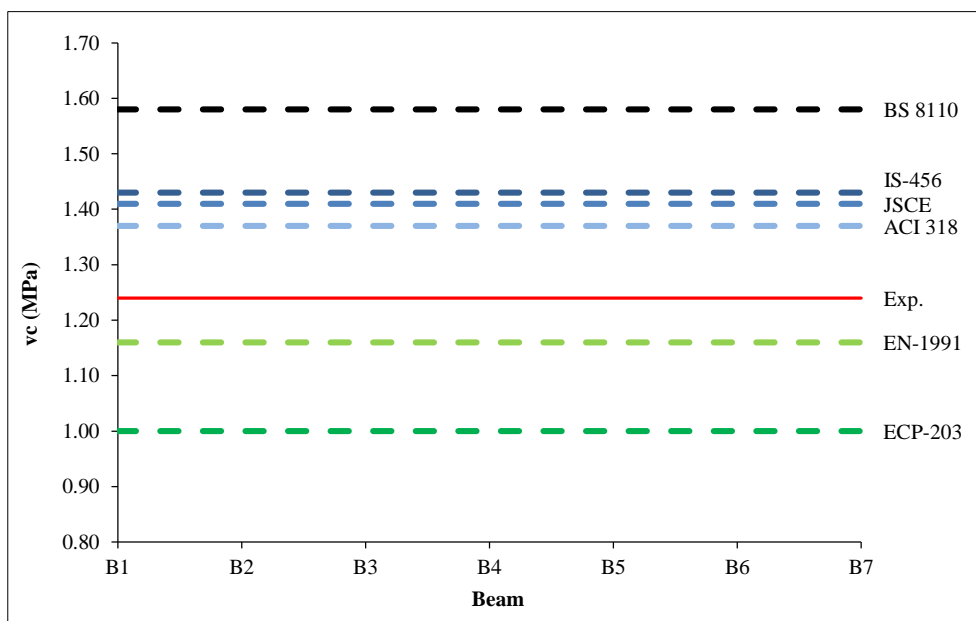


Figure 6. Experimental and calculated values of v_c for all the tested specimens

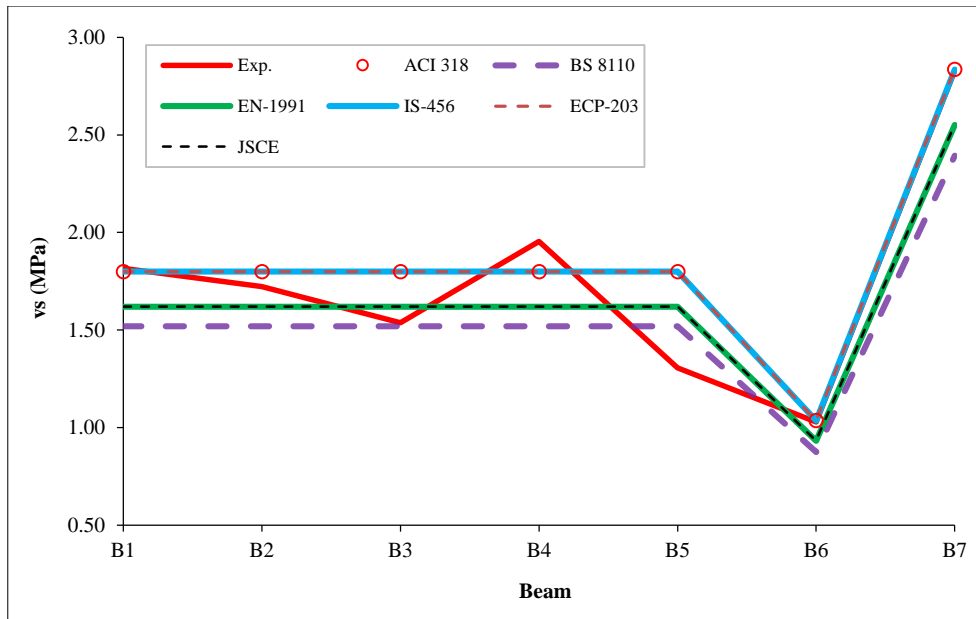


Figure 7. Experimental and calculated values of (vs) for all the tested specimens

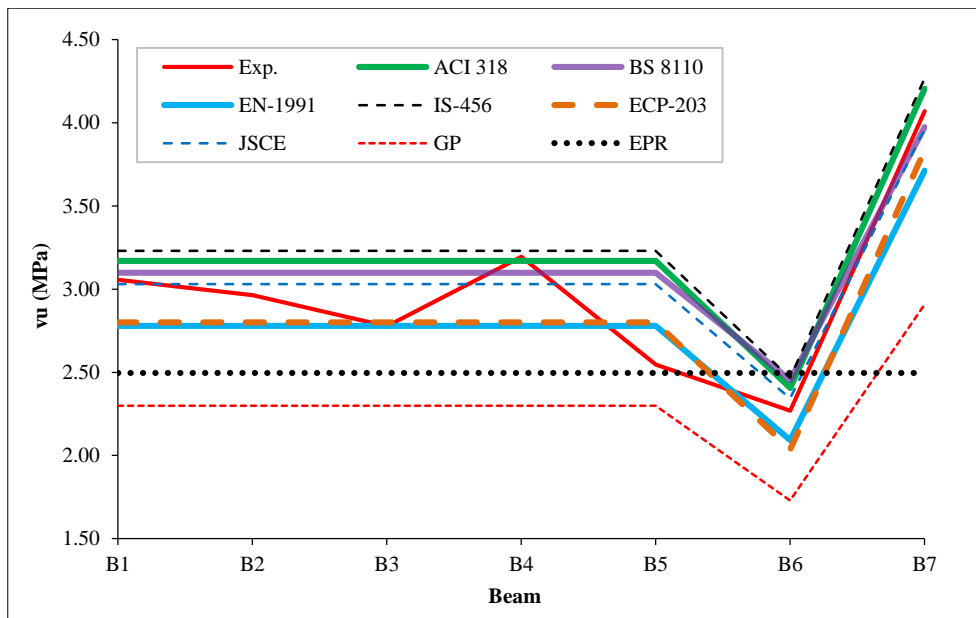


Figure 8. Experimental and calculated values of (vu) for all the tested specimens

Figure 6 compares the calculated values for the ultimate shear strength contributed by the concrete (v_c) from different design codes against the experimentally obtained values. It had been shown that the Egyptian Code of Practice (ECP-203) is the most conservative code, while the British Standards (BS-8110) is the least conservative one. Also, the Euro Code (EN-1991) was the closest to the experimental results. This point was previously discussed in detail in the previous part of this research [3].

Figure 7 compares the calculated values for the ultimate shear strength contributed by the reinforcement (v_s) from the same six previously mentioned design codes (although it was intended only for conventional beams) to the experimental results. The figure assured that the used shear reinforcement was fully functioning, and its experimental capacity was almost equal to the calculated ones. Another important point that could be noted by comparing the results of beams B1 to B5 is the effect of the longitudinal spacing (S) and transversal spacing (S') of the steel stirrups on the shear reinforcement capacity. This effect was neglected by all design codes, although all five beams had the same (v_s) value regardless of their (S and S') values, but the experimental values showed the shear capacity contributed by the shear reinforcement was affected by (S and S').

Finally, Figure 8 compares the calculated values for the ultimate total shear strength (v_u) calculated from the same six design codes and provisions with two AI predictive models, Genetic Programming (GP) and Evolutionary Polynomial Regression (EPR), obtained from previous studies. Figure 8 illustrates that the experimentally measured

values of the shear capacities were within the calculated range. The average values of the (calculated / measured) ratios were (108, 106, 95, 110, 95, 104, 78, and 86%) for (ACI-318, BS-8110, EN-1991, IS-456, ECP-203, JSCE, GP, and EPR), respectively. Accordingly, (IS-456) was the least conservative, (EN-1991 and ECP-203) were the most conservative, and (JSCE) was the closest to the experimental results.

5.5. Load-Deflection Relationship

The analysis approach by Ramadan et al. [42] was considered. The recorded load-deflection curves were analyzed with respect to initial stiffness (K_i), final stiffness (K_f), dissipated energy (DE), and ductility; the definitions of these terms are graphically illustrated in Figure 9. The recorded values were listed in Table 5 and graphically presented in Figure 10.

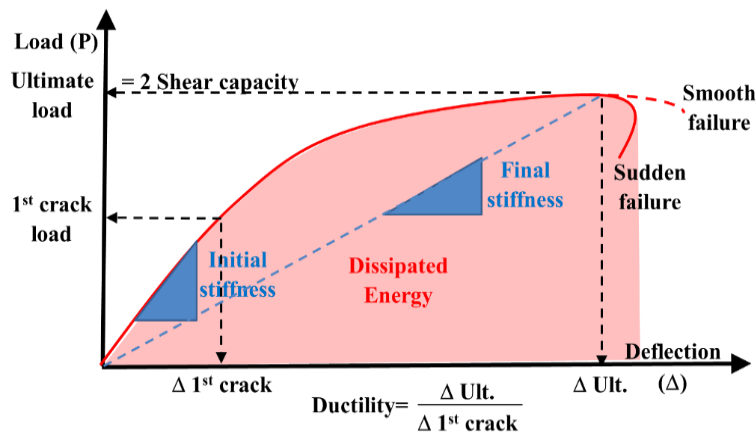
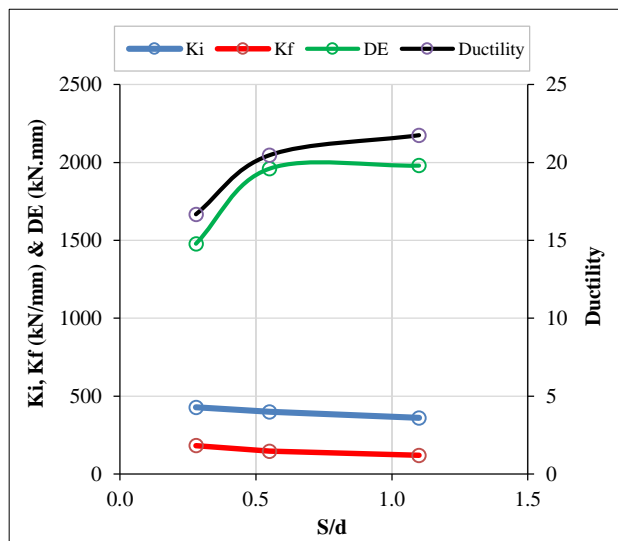


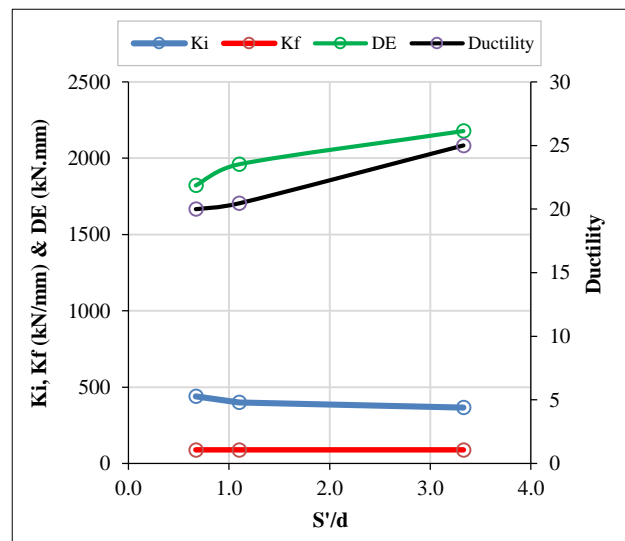
Figure 9. Load deflection curve with its parameters

Table 5. Stiffnesses and ductility of the tested wide beams

Beam	K_i (kN/mm)	K_f (kN/mm)	D.E. (kN/mm)	Ductility
B1	400	147	1960	20
B2	429	183	1478	17
B3	361	120	1980	22
B4	440	173	1822	20
B5	367	92	2178	25
B6	320	163	970	12
B7	435	160	3194	24



(a)



(b)

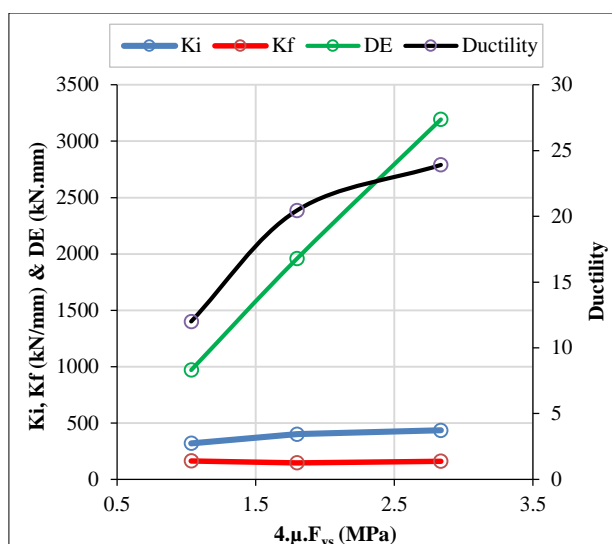


Figure 10. (Ki, Kf, DE, and Ductility) Vs a) (S/d), b) (S'/d) and c) Shear reinforcement strength

Studying the initial stiffness (Ki) (blue line) and the final stiffness (Kf) (red line) in Figure 10, a slight reduction with increasing both longitudinal and transverse spacing (S and S') and slight enhancement with increasing the amount of shear reinforcement. These observations make perfect sense because the initial and final stiffnesses depend mainly on the gross (un-cracked) and effective (cracked) inertias, respectively. The stirrups confinement has a minor preventing effect on the section cracking; hence, increasing the stirrups spacing reduces the confinement action and accordingly the stiffness, and on the other hand, increasing the shear reinforcement amount increases the confinement action and accordingly the stiffness.

Dissipated energy (DE) is a good measurement for the seismic resistance of the element (the area below the load-deflection curve), and hence, it is mainly dependent on both ultimate load and deflection values (P_u , Δ_u). Referring to Figure 7, the curves of B1 to B5 showed that narrow stirrup spacing (longitudinal or transversal) increases the ultimate load and decreases the ultimate deflections, which has some balance and has a minor effect on the (DE). Accordingly, Figure 10 showed a minor increase in the (DE) with increasing (S and S'). On the other hand, the curves of B1, B6, and B7 in Figure 7 showed that increasing the amount of shear reinforcement had increased both (P_u and Δ_u) and accordingly, it had significantly increased (DE), as illustrated in Figure 10.

Similarly, ductility is the ratio between mid-span deflection at the crack stage and the ultimate stage. Table 2 showed that all the tested beams had almost the same cracking deflection values because the cracking stage depends mainly on the un-cracked inertia, which was the same for all tested specimens; thus, the value of ductility depends mainly on the ultimate deflection value. As mentioned above, narrow stirrup spacing (longitudinal or transverse) decreases the ultimate deflections. The slight increase in ductility with the increase in spacing is clarified in Figure 10. Also, Figure 7 indicates a significant increase in the ultimate deflection with increasing the amount of shear reinforcement, which justifies the significant increase in ductility shown in Figure 10.

6. Conclusions

This research has experimentally investigated the impact of longitudinal spacing of stirrups to depth ratio (S/d), transversal spacing of stirrup's branches to depth ratio (S'/d), and the ultimate shear reinforcement stress ($\mu.F_{ys}$) on the structural behavior of shallow/wide RC beams. Seven shallow RC beams with the same dimensions and materials but with different shear reinforcement amounts and spacing were tested up to failure. The recorded results were studied, analyzed, and compared against the expressions from six design codes and two (AI) models. Based on the results of this study, the following conclusions were drawn:

- Changing the longitudinal spacing of the stirrups to the depth ratio (S/d) ranging from 0.28 to 1.1 had affected the total shear capacity of the wide beams. It was concluded that (S/d = 0.5) is the most optimum and practical ratio, as it gives an advantage of both a maximum shear capacity of the wide beam and easier execution on site.
- The transverse spacing to depth ratio (S'/d) had ranged from 0.67 to 3.3. (S'/d) ranging from 0.67 to 1.1 was the most efficient in terms of the total shear capacity of the wide RC beams; on the other hand, (S'/d) ranging from 1.1 to 3.3 had a rapid decline effect on the total shear capacity of the specimens. That reduction was at its maximum at (s'/d = 3.3) with a 21 % decrease in the total shear capacity compared to (S'/d = 0.67).
- Ultimate shear reinforcement stress ($\mu.F_{ys}$) had the most impact on the total shear capacity of the beams. As the ($\mu.F_{ys}$) increased, the total shear capacity increased by a staggering 45 %, from 0.44 to 1.21. As encouraging as

these results, it would be uneconomic to use them in construction without a certain degree of importance. The practical and economic value of $(\mu \cdot F_{ys})$ would range from 0.7 to 0.9.

- The comparison of the values of the shear capacities of the experimental results (reinforcement, concrete, and total) to the formulas and expressions of the six previously discussed codes of practice and provisions had stated that the Euro Code 2 (EN 1991) was the most accurate for the concrete contribution, while the Japanese Code (JSCE) had the best estimation for the total shear capacity of the wide beams. The provisions did not have an accurate estimation for the reinforcement shear contributions as they were not intended for the wide beams (only conventional beams), and they did not account for the transverse spacing of the stirrups. GP and EPR (AI) models were used to compare their accuracy with the actual experimental results; GP had 78% accuracy, while EPR had 86% accuracy.
- The initial stiffness, final stiffness, dissipated energy, and ductility were almost the same when (S/d) and (S'/d) ratios were changed, but they had a minor change upon changing $(\mu \cdot F_{ys})$ as the initial stiffness and the dissipated energy were noticeably increased upon increasing $(\mu \cdot F_{ys})$.

Based on these conclusions, the following recommendations are proposed:

- Further study should investigate more wide beam specimens with a wider range for (S'/d) to integrate this parameter into the design equations in code provisions.
- Conducting a comprehensive parametric study to further investigate and quantify the effects of longitudinal spacing of stirrups to depth ratio (S/d) , transversal spacing of stirrup's branches to depth ratio (S'/d) , and the ultimate shear reinforcement stress $(\mu \cdot F_{ys})$ on the structural behavior of shallow/wide RC beams.
- Developing a numerical modelling to simulate the behavior of shallow/wide RC beams under shear for further investigation of the influence of S/d , S'/d , and $\mu \cdot F_{ys}$ on the structural response and comparing the results with the experimental findings of this study.

7. Abbreviations

a	The distance from the load to the support (Shear span) (mm)	b	Beam width (mm)
d	Beam depth (mm)	L	Beam span (mm)
A_s	The area of the lower longitudinal rebars (mm^2)	A_s'	The area of the upper longitudinal rebars (mm^2)
A_{sh}	The area of the shear reinforcement (mm^2)	S	The longitudinal spacing of stirrups (mm)
S'	The transvers spacing of stirrup's branches (mm)	μ	The Shear reinforcement ratio ($A_{sh}/b \cdot S$)
F_c'	The characteristic cylinder compressive strength of the concrete (MPa)	F_y	The yield stress of the longitudinal steel rebars (MPa)
F_{ys}	The yield stress of shear reinforcement (MPa)	E_s	The elastic modulus of steel (MPa)
E_c	The elastic modulus of concrete (MPa)	P_{cr}	The test load at the first flexural crack (kN)
P_{ult}	The test load at failure (kN)	Δ_{cr}	The mid-span deflection at the first flexural crack (mm)
Δ_{ult}	The mid-span deflection at failure (mm)	q_u	The total shear strength of the beam ($V_u/b \cdot d = q_c + q_s$) (MPa)
q_c	Concrete contribution in total shear strength (MPa)	q_s	Shear reinforcement contribution in total shear strength (MPa)
q_{su}	The maximum shear reinforcement contribution in total shear strength ($\mu \cdot F_{ys}$) (MPa)	ϵ_u	Maximum strain in lower rebars at failure ($\mu\epsilon$)
$\epsilon_{u sh}$	Maximum strain in stirrups at failure ($\mu\epsilon$)	ϵ_y	Yield strain of lower rebars ($\mu\epsilon$)
ϵ_{ys}	Yield strain of stirrups ($\mu\epsilon$)	K_i	Initial stiffness of the beam (kN/mm)
K_f	Final stiffness of the beam (kN/mm)	DE	Dissipated energy (kN.mm)

8. Declarations

8.1. Author Contributions

Conceptualization, A.S., D.M., and A.E.; methodology, A.S.; validation, A.S. and A.E.; formal analysis, A.S.; investigation, A.S.; resources, A.S.; data curation, A.E.; writing—original draft preparation, A.S.; writing—review and editing, D.M.; visualization, D.M.; supervision, A.K.; project administration, A.K.; funding acquisition, A.S. All authors have read and agreed to the published version of the manuscript.

8.2. Data Availability Statement

The data presented in this study are available on request from the corresponding author.

8.3. Funding

The authors received no financial support for the research, authorship, and/or publication of this article.

8.4. Conflicts of Interest

The authors declare no conflict of interest.

9. References

- [1] Lubell A, Sherwood T, Bentz E, & Collins MP. (2004). Safe shear design of large, wide beams. *Concrete International*, 26(1), 66–78.
- [2] Sherwood, E. G., Lubell, A. S., Bentz, E. C., & Collins, M. P. (2007). One-Way Shear Strength of Thick Slabs and Wide Beams. (2006). *ACI Structural Journal*, 103(6), 794-802. doi:10.14359/18229.
- [3] Soliman, A. A., Mansour, D. M., Khalil, A. H., & Ebid, A. (2023). The Impact of Aspect Ratio, Characteristic Strength and Compression Rebars on the Shear Capacity of Shallow RC Beams. *Civil Engineering Journal (Iran)*, 9(9), 2259–2271. doi:10.28991/CEJ-2023-09-09-012.
- [4] Serna-Ros, P., Fernandez-Prada, M. A., Miguel-Sosa, P., & Debb, O. A. R. (2002). Influence of stirrup distribution and support width on the shear strength of reinforced concrete wide beams. *Magazine of Concrete Research*, 54(3), 181–191. doi:10.1680/mac.2002.54.3.181.
- [5] Wang, G., Zhu, F., & Yang, C. (2020). Experimental study on Shear behaviors of RC beams strengthened with ECC layers. *IOP Conference Series: Materials Science and Engineering*, 780(4), 042024. doi:10.1088/1757-899X/780/4/042024.
- [6] Morsy, N. S., Sherif, A. G., Shoeib, A. E., & Agamy, M. H. (2018). Experimental Study of Enhancing the Shear Strength of Hidden/Shallow Beams by Using Shear Reinforcement. *Proceedings of the 3rd World Congress on Civil, Structural, and Environmental Engineering*, Budapest, Hungary. doi:10.11159/icseem18.116.
- [7] Taha, M. G., & Abbas, A. L. (2021). Effect of Longitudinal Maximum Spacing of Shear Reinforcement for wide Reinforced Concrete Beams. *IOP Conference Series: Materials Science and Engineering*, 1076(1), 012118. doi:10.1088/1757-899x/1076/1/012118.
- [8] de Sousa, A. M. D., Lantsoght, E. O. L., & El Debs, M. K. (2021). One-way shear strength of wide reinforced concrete members without stirrups. *Structural Concrete*, 22(2), 968–992. doi:10.1002/suco.202000034.
- [9] de Sousa, A. M. D., Lantsoght, E. O. L., & El Debs, M. K. (2023). Transition between Shear and Punching in Reinforced Concrete Slabs: Review and Predictions with ACI Code Expressions. *ACI Structural Journal*, 120(2), 115–128. doi:10.14359/51738350.
- [10] de Sousa, A. M. D., Lantsoght, E. O. L., & El Debs, M. K. (2023). Failure mechanism of one-way slabs under concentrated loads after local reinforcement yielding. *Engineering Structures*, 291, 116396. doi:10.1016/j.engstruct.2023.116396.
- [11] Moubarak, A. M. R., Elwardany, H., Abu El-hassan, K., & El-Din Taher, S. (2022). Shear strengthening of wide-shallow beams by inserted fasteners. *Engineering Structures*, 268. doi:10.1016/j.engstruct.2022.114554.
- [12] Elansary, A. A., Elnazlawy, Y. Y., & Abdalla, H. A. (2022). Shear behaviour of concrete wide beams with spiral lateral reinforcement. *Australian Journal of Civil Engineering*, 20(1), 174–194. doi:10.1080/14488353.2021.1942405.
- [13] Mohammed, A. S., Al-Zuhery, A. S. J., & Abdulkareem, B. F. (2023). An Experimental Study to Predict a New Formula for Calculating the Deflection in Wide Concrete Beams Reinforced with Shear Steel Plates. *International Journal of Engineering*, 36(2), 360–371. doi:10.5829/ije.2023.36.02b.15.
- [14] Khalil, A. E. H., Etman, E., Atta, A., Baraghith, A., & Behiry, R. (2019). The Effective Width in Shear Design of Wide-shallow Beams: A Comparative Study. *KSCE Journal of Civil Engineering*, 23(4), 1670–1681. doi:10.1007/s12205-019-0830-7.
- [15] Mahmoud, S. M., Mabrouk, R. T. S., & Kassem, M. E. (2021). Behavior of RC wide beams under eccentric loading. *Civil Engineering Journal (Iran)*, 7(11), 1880–1897. doi:10.28991/cej-2021-03091766.
- [16] Ebid, A. M., & Deifalla, A. (2021). Prediction of shear strength of FRP reinforced beams with and without stirrups using (GP) technique. *Ain Shams Engineering Journal*, 12(3), 2493–2510. doi:10.1016/j.asej.2021.02.006.
- [17] Abdul-Salam, B., Farghaly, A. S., & Benmokrane, B. (2016). Mechanisms of shear resistance of one-way concrete slabs reinforced with FRP bars. *Construction and Building Materials*, 127, 959–970. doi:10.1016/j.conbuildmat.2016.10.015.
- [18] Al-Hamrani, A., & Alnahhal, W. (2022). Shear behaviour of one-way high strength plain and FRC slabs reinforced with basalt FRP bars. *Composite Structures*, 302. doi:10.1016/j.compstruct.2022.116234.
- [19] El-Sayed, A. K., Al-Zaid, R. A., Al-Negheimish, A. I., Shuraim, A. B., & Alhozaimy, A. M. (2014). Long-term behavior of wide shallow RC beams strengthened with externally bonded CFRP plates. *Construction and Building Materials*, 51, 473–483. doi:10.1016/j.conbuildmat.2013.10.055.
- [20] Conforti, A., Minelli, F., Tinini, A., & Plizzari, G. A. (2015). Influence of polypropylene fibre reinforcement and width-to-effective depth ratio in wide-shallow beams. *Engineering Structures*, 88, 12–21. doi:10.1016/j.engstruct.2015.01.037.

- [21] Odero, B. J., Mutuku, R. N., Nyomboi, T., & Gariy, Z. A. (2022). Shear Performance of Concrete Beams with a Maximum Size of Recycled Concrete Aggregate. *Advances in Materials Science and Engineering*, 6804155. doi:10.1155/2022/6804155.
- [22] Sagheer, A. M., & Tabsh, S. W. (2023). Shear Strength of Concrete Beams without Stirrups Made with Recycled Coarse Aggregate. *Buildings*, 13(1), 75. doi:10.3390/buildings13010075.
- [23] Cheng, K., Du, Y., Wang, H., Liu, R., Sun, Y., Lu, Z., & Chen, L. (2023). Experimental Study of the Shear Performance of Combined Concrete–ECC Beams without Web Reinforcement. *Materials*, 16(16), 5706. doi:10.3390/ma16165706.
- [24] Yu, Y., Zhao, X., Xu, J., Chen, C., Deresa, S., & Zhang, J. (2020). Machine Learning-Based Evaluation of Shear Capacity of Recycled Aggregate Concrete Beams. *Materials*, 13(20), 4552. doi:10.3390/ma13204552.
- [25] Lantsoght, E., van der Veen, C., & Walraven, J. (2011). Experimental Study of Shear Capacity of Reinforced Concrete Slabs. *Structures Congress 2011*, 152-163. doi:10.1061/41171(401)15.
- [26] Lantsoght, E. O. L., Van Der Veen, C., & Walraven, J. C. (2014). Shear in One-Way Slabs under Concentrated Load Close to Support. (2013). *ACI Structural Journal*, 110(2), 275-284. doi:10.14359/51684407.
- [27] Alluqmani, A. E. (2020). Effect of the transversal-spacing of stirrup-legs on the behavior and strength of shallow concealed RC beams. *Journal of Engineering, Design and Technology*, 19(4), 932–942. doi:10.1108/JEDT-06-2020-0224.
- [28] Koo, S., Shin, D., & Kim, C. (2021). Application of principal component analysis approach to predict shear strength of reinforced concrete beams with stirrups. *Materials*, 14(13), 3471. doi:10.3390/ma14133471.
- [29] Fan, X., Wang, S., & Zhang, Z. (2020). A Study of Size Effect in Shear Resistance of Reinforced Concrete Beams Based on Machine Learning. *IOP Conference Series: Earth and Environmental Science*, 455(1), 12099. doi:10.1088/1755-1315/455/1/012099.
- [30] De Domenico, D., Quaranta, G., Zeng, Q., & Monti, G. (2022). Machine-learning-enhanced variable-angle truss model to predict the shear capacity of RC elements with transverse reinforcement. *Procedia Structural Integrity*, 44, 1688–1695. doi:10.1016/j.prostr.2023.01.216.
- [31] Wakjira, T. G., Ebead, U., & Alam, M. S. (2022). Machine learning-based shear capacity prediction and reliability analysis of shear-critical RC beams strengthened with inorganic composites. *Case Studies in Construction Materials*, 16. doi:10.1016/j.cscm.2022.e01008.
- [32] Wang, S., Ma, C., Wang, W., Hou, X., Xiao, X., Zhang, Z., Liu, X., & Liao, J. J. (2023). Prediction of Failure Modes and Minimum Characteristic Value of Transverse Reinforcement of RC Beams Based on Interpretable Machine Learning. *Buildings*, 13(2), 469. doi:10.3390/buildings13020469.
- [33] Soliman, A. A., Mansour, D. M., Ebid, A., & Khalil, A. H. (2023). Shallow and Wide RC Beams, Definition, Capacity and Structural Behavior – Gap Study. *The Open Civil Engineering Journal*, 17(1), 1-11. doi:10.2174/18741495-v17-e230725-2023-28.
- [34] ACI 318-89. (2019). *Building Code Requirements for Structural Concrete*. American Concrete Institute (ACI), Michigan, United States.
- [35] BS 8110-1. (1997). *Structural use of concrete*. British Standards Institution (BSI), London, United Kingdom.
- [36] ES EN 1992-1-1. (2004). *Eurocode2: Design of concrete structures - Part 1-1: General rules and rules for buildings*. European Committee for Standardization (CEN), Brussels, Belgium.
- [37] IS 456. (2000). *Plain and Reinforced Concrete-Code of Practice (4th Ed.)*. Bureau of Indian Standards, New Delhi, India.
- [38] ECP-203. (2018). *Egyptian Code for Design and Construction of Reinforced Concrete Structures*. National Housing and Building Research Center, Cairo, Egypt.
- [39] Japan Society of Civil Engineers (JSCE). (2002). *Standard Specifications for Concrete Structures*. JSCE Guideline for Concrete No. 15, Japan Society of Civil Engineers, Tokyo, Japan.
- [40] Ebid, A. M., & Deifalla, A. (2021). Prediction of shear strength of FRP reinforced beams with and without stirrups using (GP) technique. *Ain Shams Engineering Journal*, 12(3), 2493–2510. doi:10.1016/j.asej.2021.02.006.
- [41] Ebid, A. M., Deifalla, A. F., & Mahdi, H. A. (2022). Evaluating Shear Strength of Light-Weight and Normal-Weight Concretes through Artificial Intelligence. *Sustainability (Switzerland)*, 14(21), 14010. doi:10.3390/su142114010.
- [42] Ramadan, M., Ors, D. M., Farghal, A. M., Afifi, A., Zaher, A. H., & Ebid, A. M. (2023). Punching shear behavior of HSC & UHPC post tensioned flat slabs – An experimental study. *Results in Engineering*, 17, 100882. doi:10.1016/j.rineng.2023.100882.